

**On exact integration
in the finite volume element method
on simplicial meshes**

T. V. Voitovich S. Vandewalle

Report TW 378, December 2003



Katholieke Universiteit Leuven
Department of Computer Science
Celestijnenlaan 200A – B-3001 Heverlee (Belgium)

On exact integration in the finite volume element method on simplicial meshes

T. V. Voitovich S. Vandewalle

Report TW 378, December 2003

Department of Computer Science, K.U.Leuven

Abstract

This paper considers the technological aspects of the finite volume element method for the numerical solution of partial differential equations on simplicial grids in two and three dimensions. We derive new classes of integration formulas for the exact integration of generic monomials of barycentric coordinates over different types of fundamental shapes corresponding to a barycentric dual mesh. These integration formulas constitute an essential component for the development of high-order accurate finite volume element schemes. Numerical examples are presented that illustrate the effectiveness and validity of the technology.

Keywords : numerical methods for partial differential equations, finite volume element method, barycentric coordinates, integration formulas.

AMS(MOS) Classification : 65N30

ON EXACT INTEGRATION IN THE FINITE VOLUME ELEMENT METHOD ON SIMPLICIAL MESHES

T. V. VOITOVICH* AND S. VANDEWALLE†

Abstract. This paper considers the technological aspects of the finite volume element method for the numerical solution of partial differential equations on simplicial grids in two and three dimensions. We derive new classes of integration formulas for the exact integration of generic monomials of barycentric coordinates over different types of fundamental shapes corresponding to a barycentric dual mesh. These integration formulas constitute an essential component for the development of high-order accurate finite volume element schemes. Numerical examples are presented that illustrate the effectiveness and validity of the technology.

Key words. numerical methods for partial differential equations, finite volume element method, barycentric coordinates, integration formulas.

AMS subject classifications. 65N30

1. Introduction. Finite volume element (FVE) or box methods [2, 3, 5, 7], also called control-volume finite element methods [1, 9, 11], play an important rôle in the present practice of numerically solving partial differential equations (PDEs). From the finite element method, they inherit the use of piecewise polynomial finite element spaces for the representation of the solution, the PDE coefficients and source functions. Another feature rooted in the finite element context is the suitability for use with general and irregular grids, allowing the effective treatment of complex geometries, with a natural realization of local grid refinement and adaptivity. From the finite volume method, they inherit a natural discrete conservation property, the simplicity of approximation and the applicability of one-dimensional upwind schemes.

The FVE method was created to generalize and systematize the use of piecewise polynomial finite element spaces for discretization in the classical finite volume method. The FVE method starts with a partitioning of the computational domain into a set of finite elements, and the subsequent definition of a dual finite volume mesh superimposed on the finite element grid. For every finite volume the method writes out the integral conservation form of the PDE. Using the finite element representation of the solution, a discrete set of linear or nonlinear equations is then constructed. In that step, one is faced with the integration of the element-based interpolation polynomials over certain geometrical shapes defined by the dual mesh. The present paper addresses the problem of the *exact integration* of those polynomials. For a clear exposition of the FVE-method, a discussion of its use for solving problems on composite meshes, an analysis of its accuracy and a description of a multigrid approach for solving the resulting discrete set of linear equations, we refer to the monograph by McCormick [10]. An extension of these ideas towards using mixed finite elements for the simulation porous media flow, and a careful, physically motivated selection of the control volumes for this type of problem are described in [4].

Contrary to the finite element method, the technological basis of the FVE method is not well established; the integration formulas are in many cases not readily available. Such formulas are based on a local representation of the polynomials with the use of a

*Applied Mathematics Department, Novosibirsk State Technical University, 20 Karl Marx Av., 630092 Novosibirsk, Russia,

†Katholieke Universiteit Leuven, Department of Computer Science, Celestijnenlaan 200A, B-3001 Leuven, Belgium

set of basis functions and the subsequent exact integration of those basis functions over the corresponding geometrical shapes. In finite element methods on simplicial grids, the polynomial basis functions are usually expressed in terms of barycentric simplex coordinates. Then, formulas for the exact integration of the generic monomials in barycentric coordinates along an edge of a triangle, over a triangular element and over a tetrahedron, as provided, e.g., by Eisenberg and Malvern [6], are used to complete the approximation. For finite volume element discretization, a general approach for the integration of polynomial basis functions over arbitrary polygonal and polyhedral grids was given by Liu and Vinokur [8]. In their approach an arbitrary polyhedron is subdivided into a union of tetrahedra, and an arbitrary polygon into a union of triangles. Hence, a triangle and a tetrahedron, and also a straight line segment, are the fundamental shapes for the exact integration. In [8], the polynomial basis functions are expressed as generalized Taylor series in terms of tensor products of the position vector. Thus, formulas for the exact integration of generic monomials in Cartesian coordinates are derived.

In our approach, we focus on simplicial grids, with triangles (2D) and tetrahedra (3D) as the fundamental elements. We consider barycentric dual meshes, also called Donald dual meshes. In the 2D case, those are constructed with the use of the barycenters of the simplices and the midpoints of the edges; in the 3D case, also the barycenters of the tetrahedron sides are involved. We will adopt the finite element practice to express the polynomial basis functions in terms of barycentric coordinates. There is simple relationship between the basis functions and the barycentric coordinates. This enables an easy evaluation of the necessary FVE integrals, once a set of formulas for the integration of barycentric monomials is available. Here, we will derive new classes of such integration formulas. No prior subdivision of the integration domains into simplicial elements as in [8] will be required. Our fundamental integration domains will be barycentric subdomains of a 2D or 3D simplex, parts of median planes or median segments, and parts of boundary faces or edges.

The paper will extend the previous work of the first author [12]. There, for the 2D case, formulas for the integration of monomials of the first and second order were derived on the basis of geometrical observations. In the present paper a new and much more general procedure is developed for the derivation of the values of more general integrals, in both 2D and 3D settings.

The paper is organized as follows. First, in §2, we recall the basic principles behind the finite volume element method, and illustrate its application for solving partial differential equations on simplicial grids. The integrals required in the discretization procedure are derived. In §3, the formulas for the exact integration of monomials are constructed for the 2D case. The 3D case is treated in §4. Finally, in §5, the use of the formulas is illustrated by means of some numerical experiments.

2. A review of the FVE method. In this section we explain the notations that are used in the paper and elaborate the main features of the proposed technology. We also identify the integrals that need to be provided for an efficient implementation of the FVE method.

2.1. FVE method basics. The FVE method is applicable to a wide range of PDEs. Here, for illustration purposes, we focus on a 2D convection-diffusion-reaction equation from fluid dynamics, of the form

$$(2.1) \quad \frac{\partial(\rho u)}{\partial t} + \nabla \cdot (\mathbf{J}^c + \mathbf{J}^d) + \gamma u = f_u \quad \text{in } \Omega_T,$$

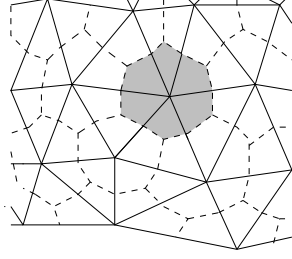


FIGURE 2.1. Fragment of finite element (solid) and control volume (dashed) meshes.

where $\Omega_T = \Omega \times (0, T)$ is the space time cylinder, with Ω a bounded domain. \mathbf{J}^c and \mathbf{J}^d are the convective and diffusive fluxes of u :

$$\mathbf{J}^c = \rho \mathbf{v} u, \quad \mathbf{J}^d = -\lambda \nabla u,$$

ρ is the fluid density, \mathbf{v} is the velocity vector, λ is the diffusion coefficient, and f_u is the volumetric source of u . Let \mathcal{T}_h be a conforming triangulation of Ω , such that the intersection of the closures of two distinct triangles is either empty or consists of one common vertex or edge. We will assume that computational points and finite element vertices coincide (the “cell-vertex” arrangement). We consider a dual mesh constructed on the centroids of the triangles and the mid-points of the edges, the so-called barycentric dual mesh or Donald dual mesh. Each vertex i has a corresponding “complete” finite volume Ω_i bounded by median segments (in the case of an interior vertex), or an “incomplete” finite volume bounded by median segments and boundary edges (in the case of a boundary vertex), see Fig. 2.1. For every Ω_i , the integral conservation form of PDE (2.1) is written as follows

$$(2.2) \quad \int_{\Omega_i} \frac{\partial(\rho u)}{\partial t} d\Omega + \int_{\partial\Omega_i} (\mathbf{J}^c + \mathbf{J}^d) \cdot \mathbf{n} ds + \int_{\Omega_i} \gamma u d\Omega = \int_{\Omega_i} f_u d\Omega,$$

where \mathbf{n} is the outward unit normal to $\partial\Omega_i$, the boundary of Ω_i .

For the representation of the FVE solution, we consider the usual finite element space of continuous piecewise polynomial functions

$$(2.3) \quad S^h = \{v \in C^0(\bar{\Omega}) \mid v|_T \in P_1 \quad \forall T \in \mathcal{T}^h\},$$

where P_1 is the space of first degree polynomials in two variables. Finite element space (2.3) can also be used for the representation of spatially varying PDE coefficients and source functions. We shall assume that the FVE solution u^h belongs to the space S_E^h ,

$$(2.4) \quad S_E^h = \{v \in S^h \mid v|_{\Gamma^D} = g^D\},$$

where Γ^D is the part of the boundary with Dirichlet boundary condition; g^D is the corresponding function. The basis $\{\psi_i(\mathbf{x})\}_{i=1}^N$ of the discrete space S^h consists of continuous piecewise linear functions $\psi_i(\mathbf{x})$ over the triangulation \mathcal{T}^h equal to 1 at vertex \mathbf{x}_i and 0 at the other vertices: $\psi_i(\mathbf{x}_j) = \delta_{ij}$, $i, j = 1, \dots, N$.

The representation of u^h restricted to one particular element $T \in \mathcal{T}^h$, is:

$$u^h(\mathbf{x}) = \sum_{m=1}^3 \hat{u}_m \hat{\psi}_m(\mathbf{x}) = a_u + b_u x + c_u y, \quad \mathbf{x} \in T,$$

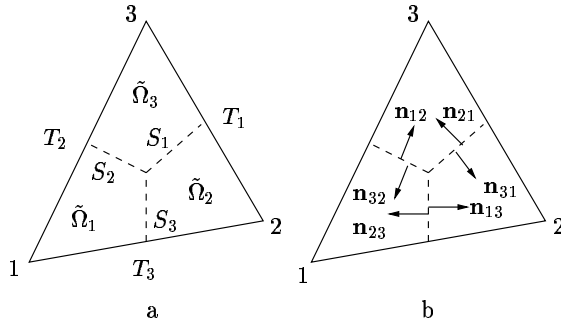


FIGURE 2.2. Graphical illustration of the key notations used in the text.

where $\hat{\psi}_m(\mathbf{x})$ are local linear basis functions. The coefficients a_u, b_u, c_u can be expressed in terms of the discrete nodal unknowns $\hat{u}_1, \hat{u}_2, \hat{u}_3$ via the inverse of the Vandermonde matrix containing the coordinates of the triangular nodes:

$$(2.5) \quad \begin{bmatrix} a_u \\ b_u \\ c_u \end{bmatrix} = \begin{bmatrix} 1 & x_1 & y_1 \\ 1 & x_2 & y_2 \\ 1 & x_3 & y_3 \end{bmatrix}^{-1} \begin{bmatrix} \hat{u}_1 \\ \hat{u}_2 \\ \hat{u}_3 \end{bmatrix} = \begin{bmatrix} k_{11} & k_{12} & k_{13} \\ k_{21} & k_{22} & k_{23} \\ k_{31} & k_{32} & k_{33} \end{bmatrix} \begin{bmatrix} \hat{u}_1 \\ \hat{u}_2 \\ \hat{u}_3 \end{bmatrix}.$$

The finite volume element method entails the numerical approximation of the integral form (2.2) over each complete or incomplete finite volume Ω_i of the dual mesh. The computation of these integrals can be organized in an element by element fashion, as in the classical finite element method. To that end, we introduce some more notations. Consider a finite element $T \in \mathcal{T}_h$. Let S_k denote a segment of the dual mesh lying on a median which emanates from the vertex k , and let Ω_l denote the barycentric subdomain of the triangle, adjacent to node l ; we will use T_i to denote the side of the triangle, opposite to node i (Fig. 2, a). The integrals in (2.2) defined over the dual mesh finite volume can be decomposed into element-wise contributions over barycentric subdomains of the form $\tilde{\Omega}_l$. The flux integrals over the boundary $\partial\tilde{\Omega}_l$ can be decomposed into element by element contributions over median segments and boundary edges. We shall denote by $J_{\nu k}$, for $\nu, k = 1, 2, 3$ the value of the combined convection-diffusion flux through the median segment S_k in the direction of $\mathbf{n}_{\nu k}$, the outward unit normal to the boundary of $\tilde{\Omega}_\nu$ (Fig. 2, b):

$$J_{\nu k} = \int_{S_k} (\mathbf{J}_{\nu k}^d + \mathbf{J}_{\nu k}^c) \cdot \mathbf{n}_{\nu k} ds.$$

It will be sufficient to approximate three of the six introduced fluxes for the element of interest. Because of the conservation property, we have that

$$J_{21} = -J_{31}, \quad J_{13} = -J_{23}, \quad J_{32} = -J_{12}.$$

We shall refer to J_{21}, J_{13}, J_{32} as the determining fluxes of the element of interest.

Note that for convection dominated problems the straightforward use of the solution space S_E^h for the approximation of convection fluxes leads to oscillatory numerical results, and up-winding or another stabilization is required. This topic is beyond the scope of the present paper. Instead, we wish to refer interested readers to [12, 13].

2.2. Integral approximation using barycentric coordinates. For the computation of the diffusion fluxes, we are faced with integrals over S_k , a segment of the dual Donald mesh:

$$(2.6) \quad J_{\nu k}^d = - \int_{S_k} \lambda \nabla u \cdot \mathbf{n}_{\nu k} ds = - \nabla u \cdot \mathbf{n}_{\nu k} \int_{S_k} \lambda ds.$$

Equivalently, the diffusion flux can be written as

$$(2.7) \quad J_{\nu k}^d = - \int_{S_k} \lambda \nabla u \cdot \mathbf{n}_{\nu k} ds = - \int_{S_k} \lambda \frac{\partial u}{\partial x} dy - \lambda \frac{\partial u}{\partial y} dx,$$

in which case the segment S_k is to be traversed in the ‘anti-clockwise’ direction w.r.t. normal $\mathbf{n}_{\nu k}$. (When looking in the direction of the normal on S_k , the segment is traversed from the right to the left.)

Discrete space (2.3) will be used for the local representation of the variable diffusion coefficient. I.e., we shall write $\lambda(\mathbf{x})$ as a linear combination of the local basis functions $\hat{\psi}_m(\mathbf{x})$, or, equivalently, we can represent the interpolation function for the diffusion coefficient in terms of barycentric (area) coordinates:

$$\lambda(\mathbf{x}) = \sum_{m=1}^3 \hat{\lambda}_m \hat{\psi}_m(\mathbf{x}) = \sum_{i=1}^3 \hat{\lambda}_m L_m, \quad \mathbf{x} \in T,$$

where $\hat{\lambda}_m$ are the nodal values of λ . The barycentric coordinates L_1, L_2, L_3 of a point $(x, y) \in T$ satisfy $L_1 + L_2 + L_3 = 1$, together with

$$L_1 \hat{x}_1 + L_2 \hat{x}_2 + L_3 \hat{x}_3 = x, \quad \text{and} \quad L_1 \hat{y}_1 + L_2 \hat{y}_2 + L_3 \hat{y}_3 = y,$$

where (\hat{x}_i, \hat{y}_i) for $i = 1, 2, 3$ are the coordinates of the three simplex nodes. Note that the local basis functions and the barycentric coordinates coincide, i.e., $\hat{\psi}_m(\mathbf{x}) = L_m$, for $m = 1, 2, 3$ in the case of conforming linear finite elements.

Using (2.5), and $\mathbf{n}_{\nu k} = (n_{\nu k, x}, n_{\nu k, y})^T$ the approximation of the diffusion flux (2.6) becomes

$$(2.8) \quad \tilde{J}_{\nu k}^d = - \left\{ \sum_{m=1}^3 \hat{\lambda}_m \int_{S_k} L_m ds \right\} \sum_{l=1}^3 (k_{2l} n_x + k_{3l} n_y) \hat{u}_l.$$

When the alternative formulation (2.7) is used, the following expression results:

$$(2.9) \quad \tilde{J}_{\nu k}^d = - \left\{ \sum_{m=1}^3 \hat{\lambda}_m \int_{S_k} L_m dy \right\} \sum_{l=1}^3 k_{2l} \hat{u}_l + \left\{ \sum_{m=1}^3 \hat{\lambda}_m \int_{S_k} L_m dx \right\} \sum_{l=1}^3 k_{3l} \hat{u}_l.$$

To complete the approximation, one should introduce integration formulas for the integration of barycentric coordinates over the dual mesh line segments:

$$(2.10) \quad \int_{S_k} L_m ds, \quad \int_{S_k} L_m dx, \quad \int_{S_k} L_m dy, \quad k, m = 1, 2, 3.$$

These formulas can also form a basis for the upwind discretization of the convection fluxes. For example, assume that the approximation of the convection fluxes is based on a weighting of local mass fluxes with the use of upwind values of the discrete unknowns \tilde{u}_k [13]:

$$(2.11) \quad \tilde{J}_{\nu k}^c = \tilde{u}_k \int_{S_k} \rho \mathbf{v} \cdot \mathbf{n}_{\nu k} ds,$$

and \tilde{u}_k is a linear combination of the local discrete unknowns. Obviously, the local mass flux, i.e., the integral in the right-hand side of (2.11), should be calculated as exactly as possible. Assume the components of vector $\rho(\mathbf{x})\mathbf{v}(\mathbf{x})$ vary linearly over each simplex:

$$(2.12) \quad \rho(\mathbf{x})\mathbf{v}(\mathbf{x}) = \sum_{i=1}^3 \hat{\rho}_i \hat{\mathbf{v}}_i L_i,$$

where $\hat{\rho}_i$ and $\hat{\mathbf{v}}_i$ are nodal values of density and nodal velocity vectors, respectively. To complete the approximation, the values of (2.10) are then again required. Sometimes a linear representation for both the velocity and the density is considered essential, for example, in order to capture sharp gradients. Hence,

$$\rho(\mathbf{x}) = \sum_{i=1}^3 \hat{\rho}_i L_i, \quad \mathbf{v}(\mathbf{x}) = \sum_{i=1}^3 \hat{\mathbf{v}}_i L_i,$$

instead of (2.12). Now, in order to compute the fluxes in (2.11), integrals are required for monomials of the second order:

$$(2.13) \quad \int_{S_m} L_\nu L_\mu ds, \quad m, \nu, \mu = 1, 2, 3.$$

Analogously, the approximation of the reaction, source and unsteady terms requires the construction of formulas for the integration of monomials in barycentric coordinates over the barycentric subdomains of the simplices, e.g., of type,

$$(2.14) \quad \int_{\tilde{\Omega}_m} L_\nu d\Omega, \quad \text{and} \quad \int_{\tilde{\Omega}_m} L_\nu L_\mu d\Omega, \quad m, \mu, \nu = 1, 2, 3.$$

The use of a linear representation of the source term in terms of barycentric coordinates, $f_u(\mathbf{x}) = \sum_{i=1}^3 \hat{f}_i L_i$, $\mathbf{x} \in T$, requires formulas of type (2.14) (left). For the approximation of source terms that are products of two functions (would we decide to represent each function with the use of continuous linear elements), or in case the source function is locally represented as a higher order (in casu second order) polynomial, it is necessary to introduce the formulas of type (2.14) (right). Similar integrals arise also in the computation of the local FVE mass matrices, which correspond to the unsteady and reaction terms.

Finally, the FVE approximation of boundary conditions is based on formulas for the integration of barycentric coordinates over boundary edges.

2.3. Summary. The success of the use of barycentric coordinates for the exact integration of polynomials in the classical finite element method lies partly in the availability of exact integration formulas for integrals along the edges L and the area A of a triangular element, and over the volume V of a tetrahedron, see [6]:

$$(2.15) \quad \int_L L_1^a L_2^b dL = \frac{a! b!}{(a+b+1)!} |L|,$$

$$(2.16) \quad \int_A L_1^a L_2^b L_3^c dA = \frac{a! b! c!}{(a+b+c+2)!} 2|A|,$$

$$(2.17) \quad \int_V L_1^a L_2^b L_3^c L_4^d dV = \frac{a! b! c! d!}{(a+b+c+d+3)!} 6|V|.$$

Our aim is to derive similar formulas applicable to the finite volume element method. Thus, in the 2D case, we will need to derive expressions for the following three types of integrals:

$$\int_{S_k} L_1^a L_2^b L_3^c ds, \quad \int_{\tilde{\Omega}_k} L_1^a L_2^b L_3^c d\Omega, \quad \int_{\Gamma \cap \Omega_i} L_1^a L_2^b ds,$$

i.e., for the exact integration of generic monomials in simplex barycentric coordinates over dual mesh lines, over barycentric subdomains and over boundary edge segments, respectively. Those integrals will provide a technological basis on which one can construct FVE solvers, in a similar way as (2.15)–(2.17) form the basis for the development of finite element solvers.

3. Finite volume element integration in 2D.

3.1. Integration over barycentric subdomains. We start off with the exact evaluation of the integrals of the monomials of barycentric coordinates over barycentric subdomains, i.e., the integral:

$$(3.1) \quad \int_{\tilde{\Omega}_k} L_1^a L_2^b L_3^c d\Omega = \int_{\tilde{\Omega}_k} L_1^a L_2^b (1 - L_1 - L_2)^c d\Omega.$$

First, we will find the integration boundaries of the coordinates L_1, L_2 within the barycentric subregion $\tilde{\Omega}_1$. To that end, we consider the images of lines of equal value of L_1 on the planar surface $z = L_2$, where z is the coordinate direction orthogonal to the plane of the mesh (see Fig. 3.1). We also need the relationship between the barycentric coordinates on the segments of the dual mesh. This relationship has to be linear, i.e., of the form:

$$L_\nu(L_\mu) = a_{\nu\mu}^{(k)} + b_{\nu\mu}^{(k)} L_\mu \quad \text{on } S_k, \quad k, \nu, \mu = 1, 2, 3.$$

The result, with $\nu \neq \mu$, is given by:

$$(3.2) \quad \text{on } S_k : L_\nu(L_\mu) = \begin{cases} L_\mu & \text{if } \nu \neq k \text{ and } \mu \neq k, \\ 1 - L_\mu & \text{if } \nu = k, \\ \frac{1}{2}(1 - L_\mu) & \text{if } \mu = k. \end{cases}$$

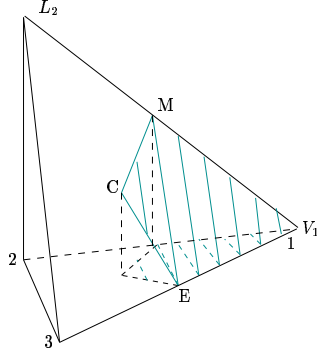


FIGURE 3.1. Limits for the integration over barycentric subdomain $\tilde{\Omega}_1$: images of the lines of equal value of the first coordinate L_1 on the surface of the second coordinate L_2 .

Using (3.2) and the expression for the differential element

$$d\Omega = 2 |T| dL_1 dL_2 ,$$

with $|T|$ the area of the triangle, one can obtain the following expression

$$(3.3) \quad \int_{\tilde{\Omega}_k} L_1^a L_2^b L_3^c d\Omega = 2 |T| \int_{\frac{1}{3}}^{\frac{1}{2}} dL_1 \int_{1-2L_1}^{L_1} L_1^a L_2^b (1-L_1-L_2)^c dL_2 \\ + 2 |T| \int_{\frac{1}{2}}^1 dL_1 \int_0^{1-L_1} L_1^a L_2^b (1-L_1-L_2)^c dL_2.$$

Here, the first integral of the right hand side corresponds to the triangle EMC and the second one to the triangle V_1ME on the surface of L_2 (see Fig. 3.1). The substitution $t = \frac{L_2}{1-L_1}$ to the right hand side integrals of (3.3) gives

$$\int_{\tilde{\Omega}_k} L_1^a L_2^b L_3^c d\Omega = 2 |T| \int_{\frac{1}{3}}^{\frac{1}{2}} L_1^a (1-L_1)^{b+c+1} \int_{\frac{1-2L_1}{1-L_1}}^{\frac{L_1}{1-L_1}} t^b (1-t)^c dt dL_1 \\ + 2 |T| \int_{\frac{1}{2}}^1 L_1^a (1-L_1)^{b+c+1} dL_1 \int_0^1 t^b (1-t)^c dt.$$

We will not attempt to evaluate the integrals in general form in terms of a, b, c . Rather, we will concentrate on the relevant cases. Calculation of the integrals for $(a, b, c) \in \{(1, 0, 0), (0, 1, 0), (0, 0, 1)\}$ gives the following result:

$$(3.4) \quad \int_{\tilde{\Omega}_k} L_\nu d\Omega = \begin{cases} \frac{11}{54} |T| & \text{if } \nu = k, \\ \frac{7}{108} |T| & \text{if } \nu \neq k. \end{cases}$$

Formula (3.4) allows a geometrical interpretation: for a fixed ν the values for $k = 1, 2, 3$ are the volumes of three truncated prisms bounded by the three barycentric subdomains $\tilde{\Omega}_k$ and the surface of the basis function L_ν , see Fig. 3.2 (right panel).

Calculation of the integrals for the monomials of second order gives

$$(3.5) \quad \int_{\tilde{\Omega}_k} L_\nu L_\mu d\Omega = \begin{cases} \frac{85}{648}|T| & \text{if } \nu = \mu = k, \\ \frac{23}{1296}|T| & \text{if } \nu = \mu \neq k, \\ \frac{47}{1296}|T| & \text{if } \nu \neq \mu \text{ and } (\nu = k \text{ or } \mu = k), \\ \frac{7}{648}|T| & \text{otherwise.} \end{cases}$$

These results are summarized in Appendix I. There, the following values are tabulated: $\frac{1}{|T|} \int_{\tilde{\Omega}_k} L_\nu L_\mu d\Omega$.

3.2. Integration over dual mesh segments. Next, we consider the exact integration of interpolation polynomials over median segments. Those integrals appear in the approximation of the convection and diffusion fluxes. We start with the computation of the following line integral:

$$\int_{S_k} L_1^a L_2^b L_3^c ds = \int_{S_k} L_1^a L_2^b (1 - L_1 - L_2)^c ds.$$

Without loss of generality, we will consider integration over segment S_1 . Let \mathbf{r} denote the position vector of a point on S_1 , and let the triangle T be defined by the points $\mathbf{r}_1, \mathbf{r}_2, \mathbf{r}_3$. Then, we have $\mathbf{r} = L_1 \mathbf{r}_1 + L_2 \mathbf{r}_2 + L_3 \mathbf{r}_3$, with $L_3 = L_2$ and $L_2 = \frac{1}{2}(1 - L_1)$, for $L_1 \in [0, 1/3]$. Thus, we find

$$ds = |\mathbf{r}'(L_1)| dL_1 = 3|S_1| dL_1,$$

where $|S_1|$ is the length of the median segment. The general expression for the differential element reads

$$(3.6) \quad \text{on } S_k : \quad ds = \begin{cases} 3|S_k| dL_\mu & \text{if } \mu = k, \\ 6|S_k| dL_\mu & \text{if } \mu \neq k. \end{cases}$$

With (3.6) and (3.2), one can integrate each of the generic monomials over the different dual mesh lines. For the first order case we have

$$\begin{aligned} \int_{S_1} L_1 ds &= \int_0^{\frac{1}{3}} L_1 |\mathbf{r}'(L_1)| dL_1 = \frac{1}{6}|S_1|, \\ \int_{S_1} L_2 ds &= \int_0^{\frac{1}{3}} \frac{1}{2} (1 - L_1) |\mathbf{r}'(L_1)| dL_1 = \frac{5}{12}|S_1|, \end{aligned}$$

and $\int_{S_1} L_2 ds = \int_{S_1} L_3 ds$. The following general rule results:

$$(3.7) \quad \int_{S_k} L_\nu ds = \begin{cases} \frac{1}{6}|S_k| & \text{if } \nu = k, \\ \frac{5}{12}|S_k| & \text{if } \nu \neq k. \end{cases}$$

For an implementation based on the ‘ dx ’, ‘ dy ’-form of the integrals, using, e.g., the expression from (2.7), formulas similar to (3.7) can be derived. For $\xi \in \{x, y\}$, we have

$$(3.8) \quad \int_{S_k} L_\nu d\xi = \begin{cases} \frac{1}{6} l_{k\xi} & \text{if } \nu = k, \\ \frac{5}{12} l_{k\xi} & \text{if } \nu \neq k. \end{cases}$$

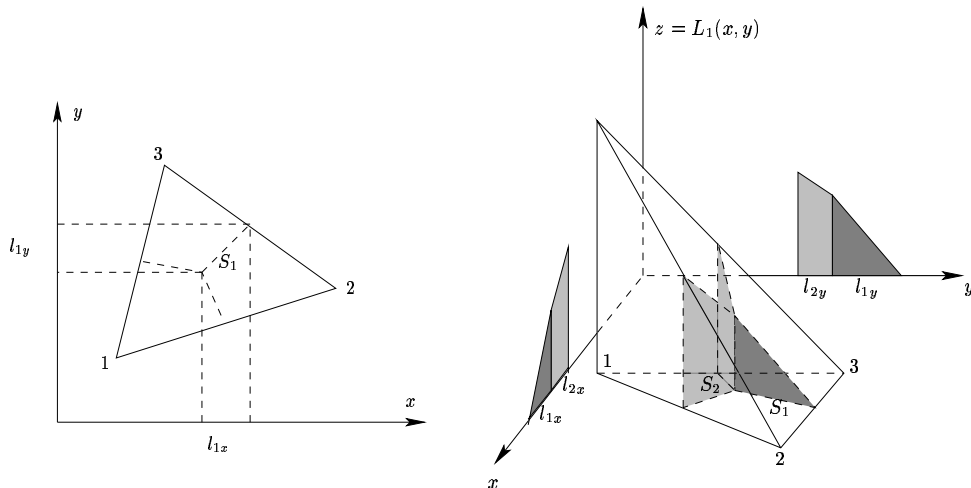


FIGURE 3.2. Integration of the barycentric coordinates over the dual mesh segments.

Here, l_{kx} and l_{ky} are the signed lengths of the projections of the median segment S_k onto the x - and y -axis, respectively, see Fig. 3.2 (left panel). In particular, we have $l_{kx} = x_{end} - x_{start}$, and $l_{ky} = y_{end} - y_{start}$. The points with coordinates (x_{start}, y_{start}) and (x_{end}, y_{end}) delineate the segment S_k , and indicate its orientation, i.e., the direction of the integration.

Formulas (3.7) and (3.8) have a simple geometrical interpretation, as illustrated in Fig. 3.2 (right panel). Consider the plane $z = L_1$, and imagine a pair of trapezoids and a triangle, constructed using the median segments and their images on the surface of that plane. The line integrals from (3.7) represent the area of the trapezoids and the triangle. Considering the value $1/3$ for L_1 at the centroid of the element and the value $1/2$ at the middle of the edges T_2 and T_3 , the correctness of (3.7) is easily verified. For (3.8), one should project the triangle onto the xz and yz coordinate planes. The area of those projections is given by $\frac{1}{6}|l_{1x}|$ and $\frac{1}{6}|l_{1y}|$, i.e., the absolute values of $\int_{S_1} L_1 dx$ and $\int_{S_1} L_1 dy$, respectively. Projection of the trapezoid corresponding to S_2 onto the same coordinate planes, gives areas of magnitude $\frac{5}{12}|l_{2x}|$ and $\frac{5}{12}|l_{2y}|$, i.e., the absolute values of integrals $\int_{S_2} L_1 dx$, $\int_{S_2} L_1 dy$, respectively. Analogous results hold for the projection of the trapezoid corresponding S_3 .

With (3.2) and (3.6), one also obtains formulas for second order monomials:

$$(3.9) \quad \int_{S_k} L_\nu L_\mu ds = \begin{cases} \frac{1}{27} |S_k| & \text{if } \nu = \mu = k, \\ \frac{7}{108} |S_k| & \text{if } \nu \neq \mu, k = \mu \text{ or } k = \nu \\ \frac{19}{108} |S_k| & \text{if } \nu \neq \mu, k \neq \mu, k \neq \nu, \end{cases}$$

where $k = 1, 2, 3$. In case ds is replaced by $d\xi$, with $\xi \in \{x, y\}$, the formulas in (3.6) need to be adapted by replacing $|S_k|$ with $l_{k\xi}$. In Appendix II, we have summarized the values of the integrals $\frac{1}{|S_k|} \int_{S_k} L_\nu L_\mu ds$.

3.3. Integration over segments of boundary edges. The FVE implementation of boundary conditions requires the exact integration of monomials over segments of boundary edges. We consider two incomplete finite volumes that share a simplex

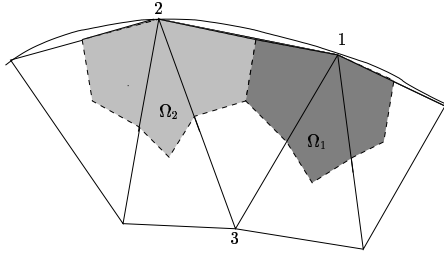


FIGURE 3.3. *Implementation of the boundary conditions: integration of the barycentric coordinates over boundary edge sections.*

T (Fig. 3.3). Let T_3 be the edge of the element that approximates the boundary and $|T_3|$ be its length. (Hence, the vertices with local numbers 1 and 2 belong to the boundary.)

For the first order monomials we have the following result:

$$(3.10) \quad \int_{\Omega_i \cap T_3} L_k ds = \begin{cases} \frac{3}{8}|T_3| & \text{if } i = k, \\ \frac{1}{8}|T_3| & \text{if } i \neq k. \end{cases}$$

Obviously, one has that $\int_{\Omega_i \cap T_3} L_3 ds = 0$, $i = 1, 2$. Similarly, one can obtain the following formulas for the integration of monomials of the second order:

$$(3.11) \quad \int_{\Omega_k \cap T_3} L_\nu^2 ds = \begin{cases} \frac{7}{24}|T_3| & \text{if } \nu = k, \\ \frac{1}{24}|T_3| & \text{if } \nu \neq k, \end{cases}$$

for $\nu \neq \mu$, one would find

$$(3.12) \quad \int_{\Omega_k \cap T_3} L_\nu L_\mu ds = \frac{1}{12}|T_3|.$$

In case in any of the above integrals ds is changed into $d\xi$, the formulas have to be adapted by changing $|T_3|$ into l_ξ , the signed length of the projection of edge T_3 onto the ξ -axis.

4. Finite volume element integration in 3D.

4.1. Introduction and notations. We consider a PDE defined on a three dimensional domain Ω . Let \mathcal{T}_h be a three dimensional triangulation of Ω : $\cup_{T_n \in \mathcal{T}_h} \bar{T}_n = \bar{\Omega}$, i.e., a set of tetrahedral elements (tetrahedrons) such that the intersection of the closures of two distinct elements is either empty or consists of one common vertex or side. As before, we will assume a cell-vertex arrangement of unknowns, i.e., the computational points and the tetrahedron vertices coincide. For the given triangulation, we construct the barycentric dual mesh, consisting of finite volumes constructed with the use of the centroids of the tetrahedral elements, the midpoints of the element edges and the centroids of the sides. Thus, any vertex of the 3D triangulation has a corresponding complete (or incomplete) control volume, bounded by parts of median planes.

Consider a tetrahedron T in \mathcal{T}_h . Let $T^{(i)}$ denote the side of the tetrahedron, that is opposite to the vertex i , with $i = 1, 2, 3, 4$. Let $\tilde{\Omega}_i$ stand for the barycentric

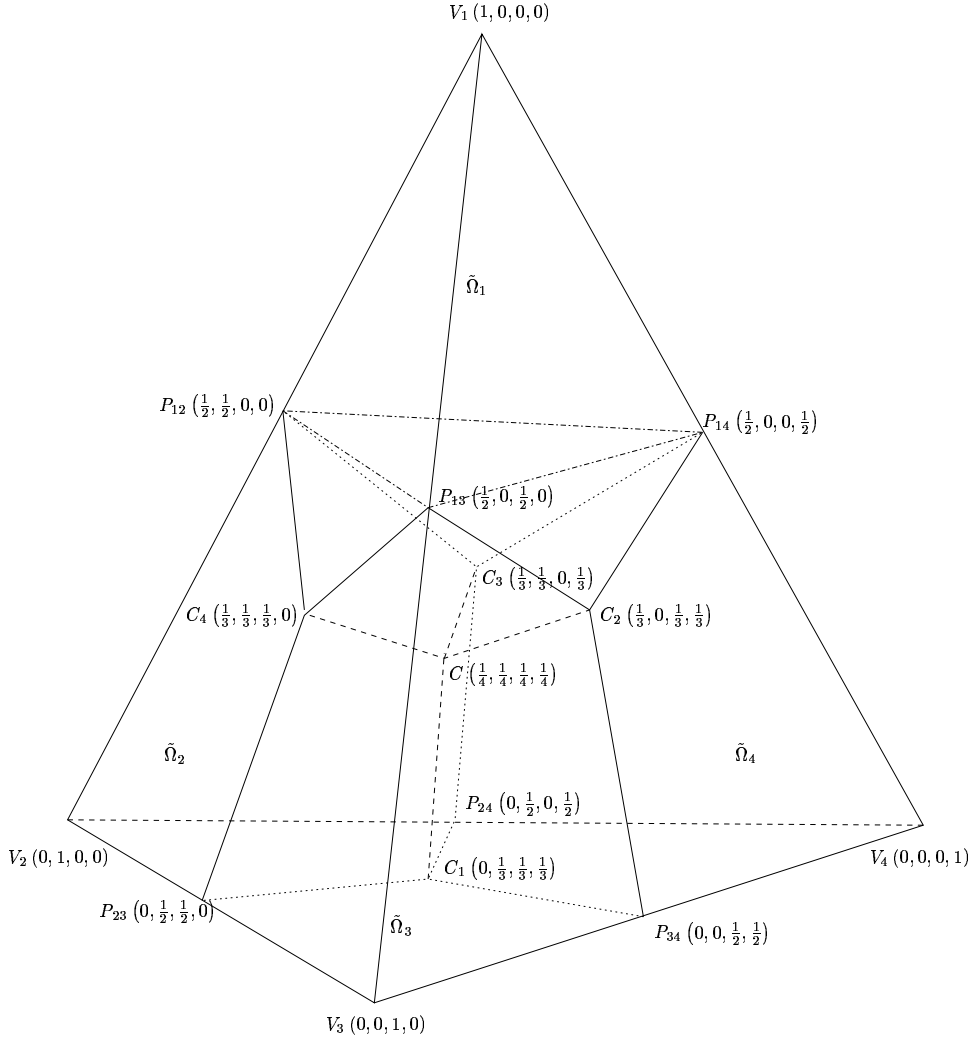


FIGURE 4.1. A tetrahedron. Indicated are the tetrahedron centroid C , the centroids of the side planes C_i , the midpoints of the edges P_{ij} and the tetrahedron vertices V_i , annotated with their barycentric coordinates. Shown also are the location of the barycentric subvolumes $\tilde{\Omega}_i$, and their side planes.

subdomain (or “quarter” element) adjacent to node i (Fig. 4.1); let E_{ij} denote the edge connecting vertices i and j ; $(\bar{x}_{ij}, \bar{y}_{ij}, \bar{z}_{ij})$ are the coordinates of the midpoint of the edge E_{ij} ; $(\hat{x}_i, \hat{y}_i, \hat{z}_i)$ are the coordinates of the barycenter of the side $T^{(i)}$; we shall use $(\hat{x}_c, \hat{y}_c, \hat{z}_c)$ to denote the coordinates of the centroid.

In this section, we are faced with the calculation of integrals of the following types: $\int_{\tilde{\Omega}_p} P(\mathbf{x}) d\Omega$, $\int_{S_p^{(q)}} P(\mathbf{x}) dS$, and $\int_{S_{pq}} P(\mathbf{x}) dS$, where $P(\mathbf{x}) = L_1^a L_2^b L_3^c L_4^d$. The region S_{pq} is a quadrilateral of the dual surface which lies on the median plane coming out of edge E_{pq} (Fig. 4.3, a); $S_p^{(q)}$ is the two dimensional barycentric subdomain of the side opposite to node q , and adjacent to node p (Fig. 4.4).

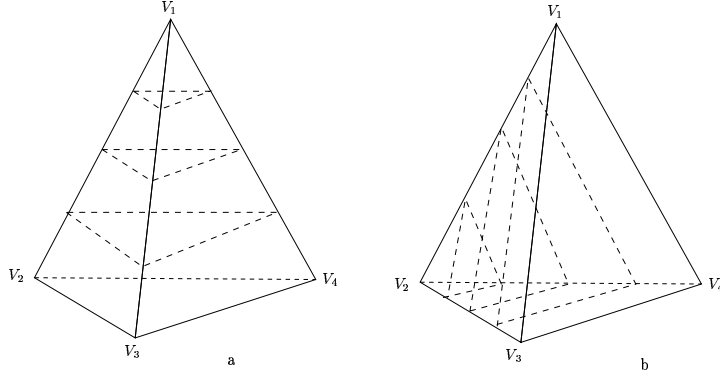


FIGURE 4.2. Planes of equal values of L_1 (a) and L_2 (b).

4.2. Integration over barycentric subdomains. For the approximation of source terms and for the evaluation of the FVE method mass matrix, one needs the following integrals, similar to (3.1),

$$(4.1) \quad \int_{\tilde{\Omega}_k} L_1^a L_2^b L_3^c L_4^d d\Omega = \int_{\tilde{\Omega}_k} L_1^a L_2^b L_3^c (1 - L_1 - L_2 - L_3)^d d\Omega.$$

Without loss of generality, we can consider the integration over barycentric subdomain $\tilde{\Omega}_1$ only. The differential element $d\Omega$ can be expressed as follows:

$$d\Omega = 6|T| dL_1 dL_2 dL_3,$$

with $|T|$ equal to the volume of the tetrahedron. As in the 2D case, the integral is split into two contributions. The first corresponds to the changes of L_1 from $\frac{1}{2}$ to 1 (the tetrahedron $V_1 P_{12} P_{13} P_{14}$, Fig. 4.1):

$$(4.2) \quad 6|T| \int_{\frac{1}{2}}^1 dL_1 \int_0^{1-L_1} dL_2 \int_0^{1-L_1-L_2} L_1^a L_2^b L_3^c (1 - L_1 - L_2 - L_3)^d dL_3.$$

The second part corresponds to the rest of the barycentric subdomain, where L_1 changes from $\frac{1}{4}$ to $\frac{1}{2}$:

$$(4.3) \quad 6|T| \int_{\frac{1}{4}}^{\frac{1}{2}} dL_1 \int_{\psi(L_1)}^{\phi(L_1)} dL_2 \int_{\kappa(L_1, L_2)}^{\chi(L_1, L_2)} L_1^a L_2^b L_3^c (1 - L_1 - L_2 - L_3)^d dL_3.$$

On its turn, the last integral is split into three contributions; the first contribution corresponds to the pyramid $C_3 C_4 P_{13} P_{14} P_{12}$, the second one to the pyramid $C_3 C_4 P_{13} P_{14} C_2$, and the last one to the tetrahedron $C_2 C_3 C_4 C$. In order to find the integration limits for each particular case, one needs to perform two steps.

First, in order to derive the functions $\kappa(L_1, L_2)$ and $\chi(L_1, L_2)$ one should find the variation of L_3 for fixed L_1 and L_2 . The image of the variation corresponds to the intersection of planes of equal values for L_1 and L_2 (see Fig. 4.2). These are lines that

are parallel to edge E_{34} . Consideration of those lines with the use of the equations for the tetrahedron sides and the median planes, leads to $\kappa(L_1, L_2)$ and $\chi(L_1, L_2)$. Second, in order to find the functions $\psi(L_1)$ and $\phi(L_1)$ for each subvolume, one should consider a projection of the subvolume onto the side T_3 (i.e., $L_3 = 0$), parallel to E_{34} (i.e., L_1 and L_2 constant). In that projection, one can find the integration limits for L_2 that correspond to a fixed value of L_1 . The projection of pyramid $C_3C_4P_{13}P_{14}P_{12}$ is triangle $C_3P_{12}P_{14}$, the projection of pyramid $C_3C_4P_{13}P_{14}C_2$ is triangle $\tilde{C}_2C_3P_{14}$, the projection of the tetrahedron $C_2C_3C_4C$ is triangle $\tilde{C}_2C_3\tilde{C}$. Here, the auxiliary points \tilde{C} and \tilde{C}_2 have the following barycentric coordinates: $\tilde{C}(\frac{1}{4}, \frac{1}{4}, 0, \frac{1}{2})$, $\tilde{C}_2(\frac{1}{3}, 0, 0, \frac{2}{3})$.

Finally, taking into consideration integral (4.2), one obtains the following result: integral (4.1), denoted as $I_{(4.1)}$, is composed of a sum of 4 terms:

$$(4.4) \quad I_{(4.1)} = 6|T| \int_{\frac{1}{2}}^1 dL_1 \int_0^{1-L_1} dL_2 \int_0^{1-L_1-L_2} L_1^a L_2^b L_3^c (1-L_1-L_2-L_3)^d dL_3 \\ + 6|T| \int_{\frac{1}{3}}^{\frac{1}{2}} dL_1 \int_{1-2L_1}^{L_1} dL_2 \int_0^{1-L_1-L_2} L_1^a L_2^b L_3^c (1-L_1-L_2-L_3)^d dL_3 \\ + 6|T| \int_{\frac{1}{4}}^{\frac{1}{3}} dL_1 \int_{1-3L_1}^{L_1} dL_2 \int_{1-2L_1-L_2}^{L_1} L_1^a L_2^b L_3^c (1-L_1-L_2-L_3)^d dL_3 \\ + 6|T| \int_{\frac{1}{3}}^{\frac{1}{2}} dL_1 \int_0^{1-2L_1} dL_2 \int_{1-2L_1-L_2}^{L_1} L_1^a L_2^b L_3^c (1-L_1-L_2-L_3)^d dL_3.$$

We will not evaluate (4.4) in terms of general a, b, c, d . Instead, we only present the results for the relevant cases. We have for the first order monomials:

$$(4.5) \quad \int_{\tilde{\Omega}_k} L_\nu d\Omega = \begin{cases} \frac{25}{192}|T| & \text{if } \nu = k, \\ \frac{23}{576}|T| & \text{if } \nu \neq k, \end{cases}$$

and for the monomials of second order,

$$(4.6) \quad \int_{\tilde{\Omega}_k} L_\nu L_\mu d\Omega = \begin{cases} \frac{83}{1152}|T| & \text{if } \nu = \mu = k, \\ \frac{161}{17280}|T| & \text{if } \nu = \mu \neq k, \\ \frac{67}{3456}|T| & \text{if } \nu \neq \mu \text{ and } (\nu = k \text{ or } \mu = k), \\ \frac{97}{17280}|T| & \text{otherwise.} \end{cases}$$

The values of the integral $\frac{1}{|T|} \int_{\tilde{\Omega}_k} L_\nu L_\mu d\Omega$ are given in Appendix III.

4.3. Integration over quadrilaterals of dual median planes. We now consider the computation of the following integral:

$$(4.7) \quad \int_{S_{pq}} L_1^a L_2^b L_3^c L_4^d dS.$$

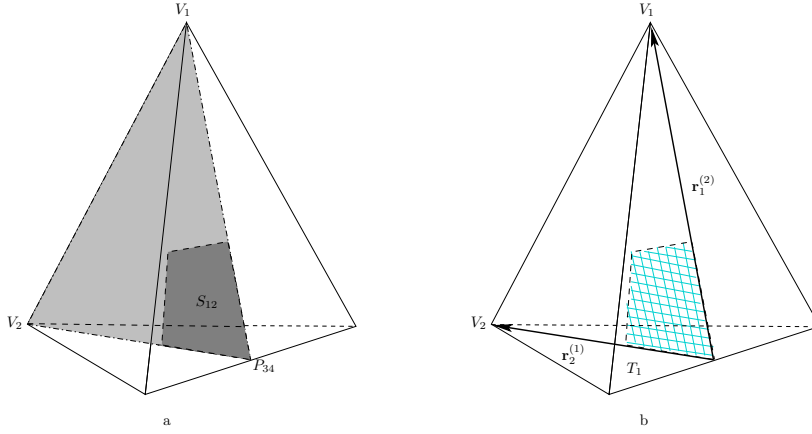


FIGURE 4.3. A median plane, emanating from edge E_{12} , and the quadrilateral part S_{12} on that plane (a); parametrization of the surface: partial derivatives of the position vector $\mathbf{r}_1^{(2)} = \partial \mathbf{r} / \partial L_1$, $\mathbf{r}_1^{(1)} = \partial \mathbf{r} / \partial L_2$ (b).

Let the tetrahedron T be defined by the four points \mathbf{r}_1 , \mathbf{r}_2 , \mathbf{r}_3 , \mathbf{r}_4 . Any position vector \mathbf{r} in the tetrahedron can be written as $\mathbf{r} = L_1 \mathbf{r}_1 + L_2 \mathbf{r}_2 + L_3 \mathbf{r}_3 + L_4 \mathbf{r}_4$, where the barycentric coordinates L_1 , L_2 , L_3 , L_4 range from 0 to 1, and satisfy $L_1 + L_2 + L_3 + L_4 = 1$. With $\mathbf{r}_i^{(k)}$, we denote the vector in the tetrahedron side $T^{(k)}$, starting at the middle of the edge opposite to node i and ending at the node i (Fig. 4.3, b).

Without loss of generality, we consider the integration over S_{12} only. We will use the barycentric coordinates L_1 and L_2 for the parametrization of that surface. Recall that $L_3 = L_4$ on the surface, hence $L_3 = (1 - L_1 - L_2) / 2$. Therefore, a point \mathbf{r} on S_{12} is given by

$$(4.8) \quad \mathbf{r} = L_1 \mathbf{r}_1 + L_2 \mathbf{r}_2 + \frac{1}{2} (1 - L_1 - L_2) (\mathbf{r}_3 + \mathbf{r}_4),$$

and the partial derivatives of the position vector with respect to L_1 , L_2 will be

$$\frac{\partial \mathbf{r}}{\partial L_1} = \mathbf{r}_1 - \frac{1}{2} (\mathbf{r}_3 + \mathbf{r}_4) = \mathbf{r}_1^{(2)}, \quad \text{and} \quad \frac{\partial \mathbf{r}}{\partial L_2} = \mathbf{r}_2 - \frac{1}{2} (\mathbf{r}_3 + \mathbf{r}_4) = \mathbf{r}_2^{(1)}.$$

Note that the vectors $\mathbf{r}_1^{(2)}$ and $\mathbf{r}_2^{(1)}$ are parallel to the barycentric coordinate lines, i.e., the lines with L_2 , resp. L_1 equal to a constant. The computation of the integrals over S_{12} requires one to find the differential element that is

$$dS = \left| \frac{\partial \mathbf{r}}{\partial L_1} \times \frac{\partial \mathbf{r}}{\partial L_2} \right| dL_1 dL_2.$$

Knowing that $\overrightarrow{P_{34}C_2} = \frac{1}{3} \mathbf{r}_1^{(2)}$, $\overrightarrow{P_{34}C_1} = \frac{1}{3} \mathbf{r}_2^{(1)}$, $\overrightarrow{P_{34}C} = \frac{1}{4} (\mathbf{r}_2^{(1)} + \mathbf{r}_1^{(2)})$ (see Fig. 4.1), one can compute the area of S_{12} to find:

$$|S_{12}| = \frac{1}{12} \left| \frac{\partial \mathbf{r}}{\partial L_1} \times \frac{\partial \mathbf{r}}{\partial L_2} \right|.$$

Therefore, the differential element is $dS = 12 |S_{12}| dL_1 dL_2$. Thus, integral (4.7) for

$(p, q) = (1, 2)$ becomes

$$\int_{S_{12}} L_1^a L_2^b L_3^c L_4^d dS = \frac{12|S_{12}|}{2^{c+d}} \int_{D_{12}} L_1^a L_2^b (1 - L_1 - L_2)^{c+d} dL_1 dL_2,$$

where D_{12} is the range of L_1, L_2 on the surface S_{12} . We find

$$(4.9) \quad \int_{S_{12}} L_1^a L_2^b L_3^c L_4^d dS = \frac{12|S_{12}|}{2^{c+d}} \int_0^{\frac{1}{4}} dL_1 \int_0^{\frac{1}{3}-\frac{1}{3}L_1} L_1^a L_2^b (1 - L_1 - L_2)^{c+d} dL_2 \\ + \frac{12|S_{12}|}{2^{c+d}} \int_{\frac{1}{4}}^{\frac{1}{3}} dL_1 \int_0^{1-3L_1} L_1^a L_2^b (1 - L_1 - L_2)^{c+d} dL_2.$$

Consider the monomials of the first order. A careful calculation of the two integrals in the right hand side of (4.9), for all the barycentric coordinates, and for the six dual quadrilaterals, leads one to the following general expression:

$$(4.10) \quad \int_{S_{pq}} L_\nu dS = \begin{cases} \frac{5}{432}|S_{pq}| & \text{if } \nu = p \text{ or } \nu = q, \\ \frac{13}{432}|S_{pq}| & \text{otherwise,} \end{cases}$$

where $|S_{pq}|$ is the area of S_{pq} . For the monomials of the second order we find:

$$\int_{S_{pq}} L_\nu L_\mu dS = \begin{cases} \frac{23}{864}|S_{pq}| & \text{if } \nu = \mu = p \text{ or } \nu = \mu = q, \\ \frac{5}{288}|S_{pq}| & \text{if } \nu = p \text{ and } \mu = q \text{ or } \mu = p \text{ and } \nu = q, \\ \frac{115}{864}|S_{pq}| & \text{if } \nu \neq p \text{ and } \nu \neq q \text{ and } \mu \neq p \text{ and } \mu \neq q, \\ \frac{41}{864}|S_{pq}| & \text{otherwise.} \end{cases}$$

These results, without the coefficient $|S_{pq}|$, are tabulated in Appendix IV.

The implementation of the FVE method may require evaluation of surface integrals written in ‘ $dy dz$ ’, ‘ $dz dx$ ’, or ‘ $dx dy$ ’-form, rather than in ‘ dS ’-notation. Such formulation is not uncommon, e.g., for the diffusion flux:

$$(4.11) \quad \int_{S_{pq}} \lambda \nabla u \cdot \mathbf{n} dS = \int_{S_{pq}} \lambda \frac{\partial u}{\partial x} dy dz + \lambda \frac{\partial u}{\partial y} dz dx + \lambda \frac{\partial u}{\partial z} dx dy.$$

In the right hand side, S_{pq} is now to be interpreted as a part of the median plane oriented by the normal \mathbf{n} . Note that one should identify a unique “determining” normal from the two normals that are associated with the median plane, to have a procedure for evaluation of local contributions of the tetrahedron onto the global discrete analogue of the problem. For example, consideration of the vector products of the vectors $\mathbf{r}_i^{(j)}$, $i, j = 1, \dots, 4$, allows one to do that: one can use the condition $j > i$ in order to select six determining normals from the set

$$\left\{ \frac{\mathbf{r}_i^{(j)} \times \mathbf{r}_j^{(i)}}{|\mathbf{r}_i^{(j)} \times \mathbf{r}_j^{(i)}|}, \quad i, j = 1, 2, 3 \right\}.$$

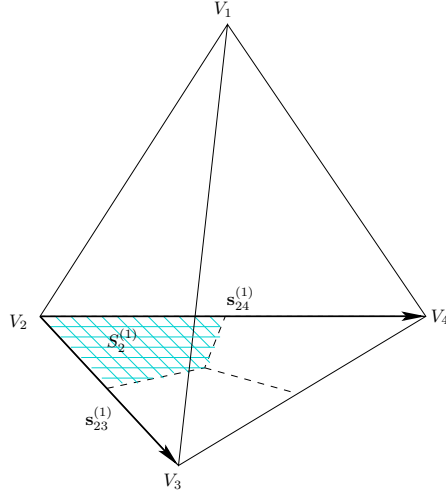


FIGURE 4.4. Implementation of boundary conditions: integration over barycentric subdomains of boundary sides; parametrization of the subdomains.

We discuss the integration over S_{12} . Assume the determining normal is chosen as $(\mathbf{r}_1^{(2)} \times \mathbf{r}_2^{(1)})/|\mathbf{r}_1^{(2)} \times \mathbf{r}_2^{(1)}|$. Let S_{12}^{yz} , S_{12}^{zx} , S_{12}^{xy} be the signed areas of the projections of S_{12} onto the yz -, zx -, and xy -coordinate planes, respectively, i.e.,

$$(4.12) \quad S_{12}^{xy} = \int_{S_{12}} dx dy,$$

with a sign corresponding to the determining normal of S_{12} . The calculation is performed with the use of a decomposition of the quadrilateral into two triangles, e.g., $S_{12} = (\triangle CP_{34}C_2) \cup (\triangle CP_{34}C_1)$ (see Fig. 4.1). We use the following order of the points in the triangles: $P_{34}CC_1$, and $P_{34}C_2C$. That is, the orientation is anticlockwise as seen from the top of the determining normal. For the signed area of the projection we will then have the following formula

$$(4.13) \quad S_{12}^{xy} = \frac{1}{2} \begin{vmatrix} 1 & \bar{x}_{34} & \bar{y}_{34} \\ 1 & x_c & y_c \\ 1 & \hat{x}_1 & \hat{y}_1 \end{vmatrix} + \frac{1}{2} \begin{vmatrix} 1 & \bar{x}_{34} & \bar{y}_{34} \\ 1 & \hat{x}_2 & \hat{y}_2 \\ 1 & x_c & y_c \end{vmatrix}.$$

Calculation of the integrals appearing in (4.11) requires one to introduce integration formulas of the following type, which are the analogues of (4.10),

$$(4.14) \quad \int_{S_{pq}} L_\nu dx dy = \begin{cases} \frac{5}{432} S_{pq}^{xy} & \text{if } \nu = p \text{ or } \nu = q, \\ \frac{13}{432} S_{pq}^{xy} & \text{otherwise.} \end{cases}$$

Here S_{pq}^{xy} is the signed area of the projection of S_{pq} onto the xy -coordinate plane, defined in a similar way as (4.12), and computed according to a formula similar to (4.13). Similar relations are valid for the “ $dy dz$ ” and “ $dz dx$ ” integrals, and also for the monomials of the second order.

4.4. Implementation of boundary conditions. The approach developed in the previous section for the calculation of the surface integrals, can also be applied

for the implementation of the boundary conditions. Let $S_k^{(i)}$ denote the barycentric subdomain of side $T^{(i)}$ adjacent to node k (see Fig. 4.4). Without loss of generality, we consider integration of monomials of the form $L_2^b L_3^c L_4^d$ over barycentric subdomain $S_2^{(1)}$. We shall use barycentric coordinates L_3 and L_4 for the parametrization of this surface. Let $\mathbf{s}_{ij}^{(\nu)}$ denote the vector in the side of the tetrahedron opposite to the node ν , directed from vertex i to vertex j . One can find that

$$\mathbf{s}_{23}^{(1)} = \partial \mathbf{r} / \partial L_3, \quad \mathbf{s}_{24}^{(1)} = \partial \mathbf{r} / \partial L_4.$$

With an argument similar to that in the previous section, and denoting by $|S_2^{(1)}|$ the area of $S_2^{(1)}$, one finds that the differential element is

$$dS = \left| \frac{\partial \mathbf{r}}{\partial L_3} \times \frac{\partial \mathbf{r}}{\partial L_4} \right| dL_3 dL_4 = 6 |S_2^{(1)}| dL_3 dL_4.$$

After determination of the integration limits, the integral of interest becomes

$$\begin{aligned} \int_{S_2^{(1)}} L_2^b L_3^c L_4^d dS &= 6 |S_2^{(1)}| \int_0^{\frac{1}{3}} dL_3 \int_0^{\frac{1}{2} - \frac{1}{2}L_3} (1 - L_3 - L_4)^b L_3^c L_4^d dL_4 \\ &+ 6 |S_2^{(1)}| \int_{\frac{1}{3}}^{\frac{1}{2}} dL_3 \int_0^{1-2L_3} (1 - L_3 - L_4)^b L_3^c L_4^d dL_4. \end{aligned}$$

Calculation of all the integrals for the monomials of the first order gives

$$(4.15) \quad \int_{S_k^{(i)}} L_\nu dS = \begin{cases} 0 & \text{if } \nu = i, \\ \frac{11}{18} |S_2^{(1)}| & \text{if } \nu = k, \\ \frac{7}{36} |S_2^{(1)}| & \text{if } \nu \neq k, \nu \neq i. \end{cases}$$

Let $S_2^{(1)yz}$, $S_2^{(1)zx}$, $S_2^{(1)xy}$ be the signed areas of the projections of subdomain $S_2^{(1)}$ onto the coordinate planes, with the sign corresponding to the normal specified in the boundary condition term. Then, formulas analogous to (4.15) and written in terms of the signed areas are valid, e.g., with dS and $|S_2^{(1)}|$ replaced by $dx dy$ resp. $S_2^{(1)xy}$.

5. Numerical experiments. Recall that the present paper extends the 2D results that were presented in [12]. Here, a new and more general procedure has been developed that one can use for a much wider class of integrals. For the two-dimensional case, the correctness of the formulas for the integration of monomials of the first order has been checked in the above reference. There, the formulas have been used for the numerical solution of convection-diffusion problems on simplicial grids.

To check the correctness of the 3D formulas, we implemented a constant coefficient and a variable coefficient diffusion problem. The former reads

$$-\frac{\partial^2 u}{\partial x^2} - \frac{\partial^2 u}{\partial y^2} - \frac{\partial^2 u}{\partial z^2} = f(x, y, z), \quad (x, y, z) \in \Omega = (0, 1) \times (0, 1) \times (0, 1),$$

where f is chosen in such a way that the exact solution is known and given by $u(x, y, z) = \sin(\pi x) \sin(\pi y) \sin(\pi z)$. Homogeneous Dirichlet boundary conditions are set at the six boundary faces.

TABLE 5.1

Constant coefficient diffusion problem: discrete L_2 and L_∞ error norms and estimated rate of convergence α .

$1/h$	$\frac{\ u-u^h\ _2}{\ u\ _2}$	α	$\frac{\ u-u^h\ _\infty}{\ u\ _\infty}$	α
10	3.04232e-2	–	3.01895e-2	–
20	7.84089e-3	1.95608	7.73328e-3	1.96493
40	1.97566e-3	1.98868	1.94514e-3	1.99121
80	4.94915e-4	1.99708	4.87039e-4	1.99777

TABLE 5.2

Variable coefficient diffusion problem: discrete L_2 and L_∞ error norms and estimated rate of convergence α .

$1/h$	$\frac{\ u-u^h\ _2}{\ u\ _2}$	α	$\frac{\ u-u^h\ _\infty}{\ u\ _\infty}$	α
10	2.27738e-4	–	2.35071e-4	–
20	5.91379e-5	1.94522	6.04551e-5	1.95916
40	1.49264e-5	1.98621	1.51472e-5	1.99681
80	3.74055e-6	1.99654	3.78890e-6	1.99920

In the numerical experiments we used sequences of embedded regular 3D triangulations of the unit cube. Our regular triangulation is the result of a domain decomposition into cubes and subsequent regular subdivision of each of those into 6 tetrahedral elements. For the local representation of the variable source function a continuous piecewise linear approximation is used, allowing us to check, e.g., the correctness of (4.5). Discrete norms of the error and corresponding values of the experimental order of convergence are given in Table 5.1. They match well with the expected value of 2.

The second model problem is defined on the same spatial domain and characterized by a variable diffusion coefficient,

$$-\nabla \cdot (\lambda(x, y, z) \nabla u) = f(x, y, z), \quad (x, y, z) \in \Omega,$$

with $\lambda(x, y, z) = 1 + x + y$. The function $f(x, y, z)$ is such that the exact solution is given by $u(x, y, z) = e^{2x} + e^{2y} + e^{2z}$. Dirichlet boundary conditions are set at all boundaries. This experiment allows us to check, among others, the validity of the formulas (4.10), for the exact integration of the barycentric coordinate monomials over the median planes. Discrete norms of the error and values of the experimental order of convergence are presented in Table 5.2. Again, they behave according to the theory, i.e., with second order convergence.

REFERENCES

- [1] B. R. Baliga and S. V. Patankar. A new finite-element formulation for convection-diffusion problems. *Numer. Heat Transfer*, 3:393–409, 1980.
- [2] R. E. Bank and D. J. Rose. Some error estimates for the box method. *SIAM J. Numer. Anal.*, 24:777–787, 1987.
- [3] Z. Cai. On the finite volume element method. *Numer. Math.*, 58:713–732, 1991.
- [4] Z. Cai, J. Jones, S.F. McCormick, and T.F. Russell. Control volume mixed finite elements. *Comp. Geosci.*, 1:289–315, 1997.
- [5] Z. Cai, J. Mandel, and S. McCormick. The finite volume element method for diffusion equations on general triangulations. *SIAM J. Numer. Anal.*, 38:392–402, 1991.

- [6] M. A. Eisenberg and L. E. Malvern. On finite element integration in natural coordinates. *Int. J. Numer. Methods Eng.*, 7:574–575, 1973.
- [7] W. Hackbusch. On first and second order box schemes. *Computing*, 41:277–296, 1989.
- [8] Y. Liu and M. Vinokur. Exact integration of polynomials and symmetric quadrature formulas over arbitrary polyhedral grids. *J. Comput. Phys.*, 140:122–148, 1998.
- [9] C. Masson, H. I. Saabas, and B. R. Baliga. Co-located equal-order control-volume finite element method for two-dimensional axisymmetric incompressible fluid flow. *Int. J. Numer. Methods Fluids*, 18:1–26, 1994.
- [10] S.F. McCormick. *Multilevel Adaptive Methods for Partial Differential Equations*. SIAM, Philadelphia, 1989.
- [11] C. Prakash and S. V. Patankar. A control volume-based finite-element method for solving the Navier-Stokes equations using equal-order velocity-pressure interpolation. *Numer. Heat Transfer*, 8:259–280, 1985.
- [12] T. V. Voitovich. *Technologies of finite volume finite element method for the solution of the convection-diffusion problems on simplicial grids*. PhD thesis, Institute of Theoretical and Applied Mechanics SB RAS, Novosibirsk, Russia, 2000.
- [13] T. V. Voitovich, O. P. Solonenko, and E. P. Shurina. On the construction of high-order-accurate upwind schemes on the compact triangulation stencils. In M. Feistauer, R. Rannacher, and K. Kozel, editors, *Numerical Modelling in Continuum Mechanics*, *Proceedings of the 4th Summer Conference held in Prague, Czech Republic, 31 July – 4 August, 2000*, pages 315–326. Matfyspress, Prague, 2001.

Appendix I: Integration of monomials of barycentric coordinates of the second order over the barycentric subdomains $\tilde{\Omega}_1, \tilde{\Omega}_2$, and $\tilde{\Omega}_3$.

$\tilde{\Omega}_1$	L_1	L_2	L_3
L_1	$\frac{85}{648}$	$\frac{47}{1296}$	$\frac{47}{1296}$
L_2	$\frac{47}{1296}$	$\frac{23}{1296}$	$\frac{7}{648}$
L_3	$\frac{47}{1296}$	$\frac{7}{648}$	$\frac{23}{1296}$

$\tilde{\Omega}_2$	L_1	L_2	L_3
L_1	$\frac{23}{1296}$	$\frac{47}{1296}$	$\frac{7}{648}$
L_2	$\frac{47}{1296}$	$\frac{85}{648}$	$\frac{47}{1296}$
L_3	$\frac{7}{648}$	$\frac{47}{1296}$	$\frac{23}{1296}$

$\tilde{\Omega}_3$	L_1	L_2	L_3
L_1	$\frac{23}{1296}$	$\frac{7}{648}$	$\frac{47}{1296}$
L_2	$\frac{7}{648}$	$\frac{23}{1296}$	$\frac{47}{1296}$
L_3	$\frac{47}{1296}$	$\frac{47}{1296}$	$\frac{85}{648}$

Appendix II: Integration of monomials of barycentric coordinates of the second order over the median segments $\mathbf{S}_1, \mathbf{S}_2$, and \mathbf{S}_3 .

\mathbf{S}_1	L_1	L_2	L_3
L_1	$\frac{1}{27}$	$\frac{7}{108}$	$\frac{7}{108}$
L_2	$\frac{7}{108}$	$\frac{19}{108}$	$\frac{19}{108}$
L_3	$\frac{7}{108}$	$\frac{19}{108}$	$\frac{19}{108}$

\mathbf{S}_2	L_1	L_2	L_3
L_1	$\frac{19}{108}$	$\frac{7}{108}$	$\frac{19}{108}$
L_2	$\frac{7}{108}$	$\frac{1}{27}$	$\frac{7}{108}$
L_3	$\frac{19}{108}$	$\frac{7}{108}$	$\frac{19}{108}$

\mathbf{S}_3	L_1	L_2	L_3
L_1	$\frac{19}{108}$	$\frac{19}{108}$	$\frac{7}{108}$
L_2	$\frac{19}{108}$	$\frac{19}{108}$	$\frac{7}{108}$
L_3	$\frac{7}{108}$	$\frac{7}{108}$	$\frac{1}{27}$

Appendix III: Integration of monomials of volumetric barycentric coordinates of the second order over barycentric subdomains $\tilde{\Omega}_1, \tilde{\Omega}_2, \tilde{\Omega}_3$, and $\tilde{\Omega}_4$.

$\tilde{\Omega}_1$	L_1	L_2	L_3	L_4
L_1	$\frac{83}{1152}$	$\frac{67}{3456}$	$\frac{67}{3456}$	$\frac{67}{3456}$
L_2	$\frac{67}{3456}$	$\frac{161}{17280}$	$\frac{97}{17280}$	$\frac{97}{17280}$
L_3	$\frac{67}{3456}$	$\frac{97}{17280}$	$\frac{161}{17280}$	$\frac{97}{17280}$
L_4	$\frac{67}{3456}$	$\frac{97}{17280}$	$\frac{97}{17280}$	$\frac{161}{17280}$

$\tilde{\Omega}_2$	L_1	L_2	L_3	L_4
L_1	$\frac{161}{17280}$	$\frac{67}{3456}$	$\frac{97}{17280}$	$\frac{97}{17280}$
L_2	$\frac{67}{3456}$	$\frac{83}{1152}$	$\frac{67}{3456}$	$\frac{67}{3456}$
L_3	$\frac{97}{17280}$	$\frac{67}{3456}$	$\frac{161}{17280}$	$\frac{97}{17280}$
L_4	$\frac{97}{17280}$	$\frac{67}{3456}$	$\frac{97}{17280}$	$\frac{161}{17280}$

$\tilde{\Omega}_3$	L_1	L_2	L_3	L_4
L_1	$\frac{161}{17280}$	$\frac{97}{17280}$	$\frac{67}{3456}$	$\frac{97}{17280}$
L_2	$\frac{97}{17280}$	$\frac{161}{17280}$	$\frac{67}{3456}$	$\frac{97}{17280}$
L_3	$\frac{67}{3456}$	$\frac{67}{3456}$	$\frac{83}{1152}$	$\frac{67}{3456}$
L_4	$\frac{97}{17280}$	$\frac{97}{17280}$	$\frac{67}{3456}$	$\frac{161}{17280}$

$\tilde{\Omega}_4$	L_1	L_2	L_3	L_4
L_1	$\frac{161}{17280}$	$\frac{97}{17280}$	$\frac{97}{17280}$	$\frac{67}{3456}$
L_2	$\frac{97}{17280}$	$\frac{161}{17280}$	$\frac{97}{17280}$	$\frac{67}{3456}$
L_3	$\frac{97}{17280}$	$\frac{97}{17280}$	$\frac{161}{17280}$	$\frac{67}{3456}$
L_4	$\frac{67}{3456}$	$\frac{67}{3456}$	$\frac{67}{3456}$	$\frac{83}{1152}$

Appendix IV: Integration of monomials of volumetric barycentric coordinates of second order over parts of median planes: \mathbf{S}_{12} , \mathbf{S}_{13} , \mathbf{S}_{14} , \mathbf{S}_{23} , \mathbf{S}_{24} , and \mathbf{S}_{34} .

\mathbf{S}_{12}	L_1	L_2	L_3	L_4
L_1	$\frac{23}{10368}$	$\frac{5}{3456}$	$\frac{41}{10368}$	$\frac{41}{10368}$
L_2	$\frac{5}{3456}$	$\frac{23}{10368}$	$\frac{41}{10368}$	$\frac{41}{10368}$
L_3	$\frac{41}{10368}$	$\frac{41}{10368}$	$\frac{115}{10368}$	$\frac{115}{10368}$
L_4	$\frac{41}{10368}$	$\frac{41}{10368}$	$\frac{115}{10368}$	$\frac{115}{10368}$

\mathbf{S}_{13}	L_1	L_2	L_3	L_4
L_1	$\frac{23}{10368}$	$\frac{41}{10368}$	$\frac{5}{3456}$	$\frac{41}{10368}$
L_2	$\frac{41}{10368}$	$\frac{115}{10368}$	$\frac{41}{10368}$	$\frac{115}{10368}$
L_3	$\frac{5}{3456}$	$\frac{41}{10368}$	$\frac{23}{10368}$	$\frac{41}{10368}$
L_4	$\frac{41}{10368}$	$\frac{115}{10368}$	$\frac{41}{10368}$	$\frac{115}{10368}$

\mathbf{S}_{14}	L_1	L_2	L_3	L_4
L_1	$\frac{23}{10368}$	$\frac{41}{10368}$	$\frac{41}{10368}$	$\frac{5}{3456}$
L_2	$\frac{41}{10368}$	$\frac{115}{10368}$	$\frac{115}{10368}$	$\frac{41}{10368}$
L_3	$\frac{41}{10368}$	$\frac{115}{10368}$	$\frac{115}{10368}$	$\frac{41}{10368}$
L_4	$\frac{5}{3456}$	$\frac{41}{10368}$	$\frac{41}{10368}$	$\frac{23}{10368}$

\mathbf{S}_{23}	L_1	L_2	L_3	L_4
L_1	$\frac{115}{10368}$	$\frac{41}{10368}$	$\frac{41}{10368}$	$\frac{115}{10368}$
L_2	$\frac{41}{10368}$	$\frac{23}{10368}$	$\frac{5}{3456}$	$\frac{41}{10368}$
L_3	$\frac{41}{10368}$	$\frac{5}{3456}$	$\frac{23}{10368}$	$\frac{41}{10368}$
L_4	$\frac{115}{10368}$	$\frac{41}{10368}$	$\frac{41}{10368}$	$\frac{115}{10368}$

\mathbf{S}_{24}	L_1	L_2	L_3	L_4
L_1	$\frac{115}{10368}$	$\frac{41}{10368}$	$\frac{115}{10368}$	$\frac{41}{10368}$
L_2	$\frac{41}{10368}$	$\frac{23}{10368}$	$\frac{41}{10368}$	$\frac{5}{3456}$
L_3	$\frac{115}{10368}$	$\frac{41}{10368}$	$\frac{115}{10368}$	$\frac{41}{10368}$
L_4	$\frac{41}{10368}$	$\frac{5}{3456}$	$\frac{41}{10368}$	$\frac{23}{10368}$

\mathbf{S}_{34}	L_1	L_2	L_3	L_4
L_1	$\frac{115}{10368}$	$\frac{115}{10368}$	$\frac{41}{10368}$	$\frac{41}{10368}$
L_2	$\frac{115}{10368}$	$\frac{115}{10368}$	$\frac{41}{10368}$	$\frac{41}{10368}$
L_3	$\frac{41}{10368}$	$\frac{41}{10368}$	$\frac{23}{10368}$	$\frac{5}{3456}$
L_4	$\frac{41}{10368}$	$\frac{41}{10368}$	$\frac{5}{3456}$	$\frac{23}{10368}$